Dimensioning of Point Absorbers for Wave Energy Conversion by Means of Differential Evolutionary Algorithms

M. BLANCO, M. LAFOZ, D. RAMIREZ, G. NAVARRO, J. TORRES AND L. GARCÍA-TABARES

This is an "Accepted article" version of a paper and it is not the "Final published article" version as appearing in IEEE Transactions on Sustainable Energy (Volume: 10, Issue: 3, July 2019).and published on 26 July 2018.

How to Cite this article:

M. Blanco, M. Lafoz, D. Ramirez, G. Navarro, J. Torres and L. García-Tabares, "Dimensioning of Point Absorbers for Wave Energy Conversion by Means of Differential Evolutionary Algorithms," in IEEE Transactions on Sustainable Energy, vol. 10, no. 3, pp. 1076-1085, July 2019, doi: 10.1109/TSTE.2018.2860462.

DOI: https://doi.org/10.1109/TSTE.2018.2860462

Dimensioning of Point Absorbers for Wave Energy Conversion by means of Differential Evolutionary Algorithms

M. Blanco, M. Lafoz, D. Ramirez, *Senior Member*, *IEEE*, G. Navarro, J. Torres, L. García-Tabares

***Abstract*—The dimensioning of the prime mover of a wave energy converter (WEC) is a key step in the entire WEC design process. The paper presents an automatic optimization methodology that focusses on the preliminary dimensioning of a point absorber WEC. By means of the proposed methodology, the engineering problem of dimensioning a WEC becomes a mathematic optimization problem. The methodology is based on a multi-objective differential evolutionary (DE) algorithm which optimizes the geometry of a heaving 2-body point absorber WEC where the Power Take-Off (PTO), its control and location are pre-selected. The algorithm considers two cost functions (WEC surface and annual energy extraction) and several constraints related to PTO characteristics or wave climate. The paper proposes a case study based on a real WEC development project in order to present the methodology. In addition, the impact on the results of the definition of the optimization problem is evaluated. The changes in cost functions and constraints evaluated have led to different geometry solutions. This automatic methodology could be easily integrated in the entire WEC design process providing a set of properly selected base cases to focus on the detail engineering, among other potential applications.**

***Index Terms*— Ocean Wave Energy, WEC Point Absorber, Direct-Drive PTO, Design methodology, Differential Evolution Optimization methods**

I. NOMENCLATURE

t	Iteration number of the optimization algorithm
P_t	Initial candidate-solutions set in the iteration t
Q_t	Trial-solutions set in the iteration t
T_p (s)	Wave peak period
H_s (m)	Significant wave height
$T_{-1,0}$ (s)	Wave energy period
J_w (W/m)	Wave power per unit of wave front
E_w (W/m)	Wave energy stored per unit area of sea surface
OP (%)	Occurrence probability of a sea-state
T_{min} (s)	Minimum wave period where the WEC is active
T_{max} (s)	Maximum wave period where the WEC is active
T_{nom} (s)	Most probable sea-sate wave period.
A (m)	Wave amplitude
ω (rad/s)	Wave angular velocity
T (s)	Wave period
$\blacksquare_1$	Sub-index *1* stands for the float body 1.
$\blacksquare_2$	Sub-index *2* stands for the submerged body 2.
$\hat{\blacksquare}$	Phasor expressed as a complex number
$\lvert\blacksquare\rvert$	Stands the module of a complex number
$\theta_{\blacksquare}$	Stands the angle of a complex number
$*$	Convolution product
j	Complex coefficient (equal to $\sqrt{-1}$)
$\hat{v}_i$ (m/s)	Vertical velocity of the body i
$\hat{v}_r$ (m/s)	Relative velocity between the two bodies
$\hat{s}_i$ (m)	Vertical displacement of the body i
$\hat{s}_r$ (m)	Relative displacement between the two bodies
R_{rii} (Kg/s)	Radiation damping coefficient
m_{adii} (Kg)	Added mass
$\hat{f}_{e,i}$ (N/m)	Excitation coefficient
$R_{v,i}$ (Kg/s)	Mechanical additional dissipative damping
S_i (Kg/s[2])	Hydrostatic restoring coefficient
Z_i (Kg/s)	Total mechanical impedance
$\hat{F}_{PTO}$ (N)	Mechanical force exerted by the generator.
P_{elect} (W)	Mean electric power generated by the PTO
P_e (W)	Mechanical power
P_{cu} (W)	SRLG cupper power losses
R (Ω)	Winding electrical resistance
I_{nom} (A)	Nominal current of the linear electric generator
R' (Kg/s)	PTO Loss Impedance
$\hat{F}_T$ (N)	*Thevenin* equivalent force
Z_T (Kg/s)	*Thevenin* equivalent impedance
S_{WEC}	Total surface of the WEC
E (Wh)	WEC annual energy extracted
T_r (s)	WEC natural resonant period
K_p, K_v, K_s, K_r, K_{sl}, K_{he}	Relaxing coefficient of the optimization problem constraints
D_1 (m)	External diameter of floating cylinder body 1
D_2 (m)	External diameter of the tube of body 2
D_3 (m)	External diameter of submerged cylinder body 2
d_1 (m)	Draft of the cylinder body 1
d_2 (m)	Height of tube cylinder 2.
d_3 (m)	Height of submerged cylinder 2.
h (m)	Sea depth

II. INTRODUCTION

THE main goal when designing a wave energy converter (WEC) [1] is, like in any other industrial problem, to get an economically optimal and competitive solution. From the point of view of the WEC prime mover dimensioning and design (which defines WEC interaction with the waves, and therefore its capacity to extract energy), the most relevant costs can be considered related to the WEC surface and/or volume whereas

M. Blanco, M. Lafoz, G. Navarro, J. Torres, L. García-Tabares are with the Centro de Investigaciones Energéticas, Medioambientales y Tecnológicas (CIEMAT), Madrid, CO 28040 SPAIN (e-mail: marcos.blanco@ciemat.es; marcos.lafoz@ciemat.es).

D. Ramírez is with the Universidad Politécnica de Madrid (UPM, Madrid, CO 28006 SPAIN (e-mail: dionisio.ramirez@upm.es).

the economic profit can be considered proportional to the electric energy produced from the mechanical energy [2], [3]. In order to get a feasible WEC geometry solution, several technological constraints could be taken into account (depending on the development stage of the device) to consider the correlation between WEC geometry and design aspects such as: location; Power Take-Off (PTO) characteristics (e.g. its efficiency) and feasibility limits [4]; or wave energy extraction control concept [5], [6]. However, these objectives are usually opposing, so that the design problem can be posed and solved as a multi-objective optimization problem with constraints [7]. This requires the development of a parametric model of the WEC to be designed and to choose cost functions and constraints.

Some design procedures based on the expertise of engineers and developers have been used traditionally in WEC development projects [8]–[11]. However, WEC projects present important challenges such as control [6], climate dependency [12] and survivability, which lead to increased complexity of the design problem when considering the interdependency of aspects such as energy resource analysis, site location, prime mover geometry, structural design, PTO design and control. To solve these design problems using mathematical optimization algorithms is possible. These algorithms can be implemented in computer code in order to automate the procedure [13], [14], and they could be integrated as a part of a global design concept based in models (Model-Based Design; MBD) [15]. Approaches to automatic design procedures have been proposed by some authors [2], [3], [16]–[24], such as: design procedures focused on the PTO and energy extraction control [20], [23]; optimization of WEC (no-active) structure [17] or IPS-WEC (active) single part [16]; genetic algorithms to obtain basic dimensions of a submerged pitch WEC [3], Oscillating Water Column (OWC) point absorber [18] or pitch inertial WEC [19]; layout optimization integrated with control design [22], [25]; or the optimization of the complete water-contact surface of the WEC in order to maximize the energy extracted [2], [21].

Framed within the automatic design procedure concept, this paper describes a methodology for preliminary WEC geometry design. It is based on:

- Simplified WEC models, but considering PTO behavior and efficiency, control system and geographic location.
- Multi-objective optimization techniques to take into account costs and profits.
- Use of constraints that consider concepts such as technical feasibility or PTO general characteristics and/or initial requirements.

This methodology has been conceived as a design aiding tool and can be useful to determine candidate geometries for the outline design or the detail design process (mature technology projects) or to improve conceptual evaluation processes of a WEC (projects for the development of new concepts). Alternatively, it could be used as an aiding tool when evaluating the impact of various WEC design parameters [5]. In this work, a case study of the methodology is presented with data corresponding to a real project [26]. The result of this being that the type of prime mover, type of PTO, control-strategy of energy extraction and location were predefined in advance.

III. Evolutionary Algorithm

A Differential Evolutionary (DE) algorithm [7] has been implemented to solve the WEC dimensioning design problem tackled in this paper as a mathematical optimization problem (Fig. 1). A stochastic optimization algorithm has been chosen due to the complexity of the models and objective functions considered [2], [13], [25]. Among other suitable options (such as, Genetic Algorithm or Particle Swarm), DE has been chosen due to its simplicity, convergence speed and robustness [7], [18], [27]. These types of algorithms work with sets of solutions (populations) modified in an iterative process until some solutions that minimize the objective functions are found. The solutions will optionally fulfill a set of constraints expressed as equations or inequations. In this case, each solution is a different design of prime mover geometry of a WEC (defined by its fundamental dimensions). The design is based in models (MBD) due to the difficulty to obtain analytic expressions of the objective functions as function of the search space variables [28]. In consequence, each WEC geometry has been evaluated by means of a mathematical model (section IV) to get the values for each constraint (section V.C) and each objective function (section V.B). Therefore, the energy extracted by each different prime mover design (solution) depends on its geometric dimensions (search space). The objectives of the design problem are the optimization of the energy extracted and the minimization of the size of the prime mover design (objective functions). The Multi-Objective DE starts from a random set (population) of prime mover designs and it makes them evolve to better solutions. In addition, each prime mover geometry has to accomplish some technical limitations (constraints).

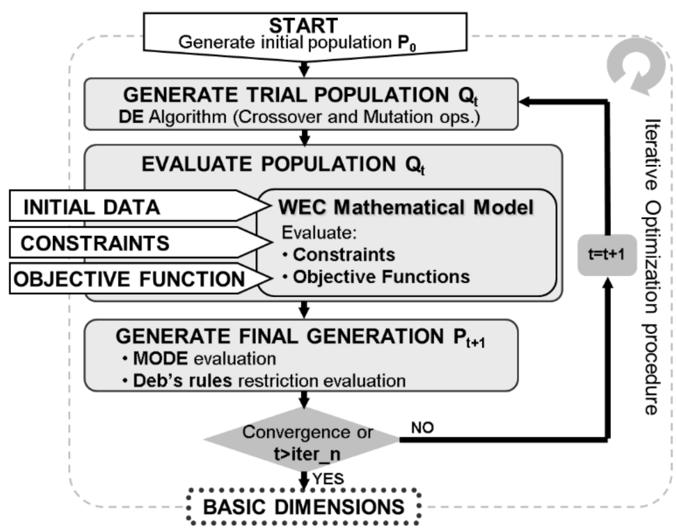

Fig. 1. General layout of the optimization problem.

A. Differential Evolutionary algorithm

The Differential Evolutionary (DE) optimization algorithm [7] repeats in each iteration *t*, the following steps,: first, a trial population of solutions (Q_t) is created from the initial population (P_t). Next, a new and potentially better set of solutions is made up of P_t and Q_t.It is named population P_{t+1}, and it is generated taking into account the objective functions and constraints. Finally, the population P_{t+1} is used in the iteration *t+1* as the initial population, and the process continues until a fixed number of iterations is reached. The Q_t set of solutions is obtained from P_t using two principal mechanisms: mutation and crossover (corresponding with the "GENERATE TRIAL SOLUTION" step shown in Fig. 1 procedure).

The foremost difference from other evolutionary algorithms is the method of mutation to generate a mutant population from P_t, by adding one solution to the weighted difference between two other randomly chosen solutions. The values used in crossover probability parameter (*Cr*) and in the differential weight parameter (*F*), are 0.9 and 0.8 respectively [7]. A maximum number of iterations (500) was fixed as the algorithm termination criterion. Constraints and *Pareto Frontier* determination correspond with the third step "GENERATE FINAL POPULATION" of the iterative procedure in Fig. 1.

B. Constraints and Multi-Objective Optimization

The tackled optimization problem needs to handle some design constraints based on *Deb*'s *Rules* [7], stating that between the two compared solutions, the one which satisfies all constraints is always chosen. If both solutions satisfy the constraints, then the value of the objective function decides which one is chosen. On the other hand, a real industrial problem has usually to manage several objective functions, such as maximising benefits or reducing costs. DE algorithm can be extended to solve multi-objective problems, converging in this case to the true *Pareto Frontier* (PF) [7]. The procedure used to obtain P_{t+1} applies two mechanisms: a non-dominated sorting finds as many *Pareto*-optimal solutions as possible; and the solutions diversity is assured by the assignment of a crowding-distance factor [7].

IV. WAVE ENERGY CONVERTER MATHEMATICAL MODEL

The prime mover used in the case study is a two-body point absorber, Fig. 4, considering a 200 kW Direct-Drive PTO (a linear electric generator) connected to the electric grid (one device, not a wave farm) located at coast of *Santoña*, *Spain*. The equations presented in this section describe the WEC dynamic behavior and allow evaluating the objective functions and constraints (section V) for each candidate solution (defined by its dimensions) considered in the algorithm.

A. Location

The chosen location is on the coast of *Santoña*, (3.46° W, 43.50° N). The sea-state is defined in standard form (according to physical oceanography) by means of two parameters [29], [30]: Significant Wave Height (H_s), defined as four times the standard deviation of the wave surface elevation (standard variable used as measurement of the height of ocean waves); and the Peak Period (T_p), defined as the period where it is the maximum of the ocean waves power spectrum or spectral density (standard variable used as measurement of the period of ocean waves). Those states at the selected location can be adjusted by a polynomial function which represents the most representative ones ($H_s=0.01438 \cdot T_p^2$). Hereinafter, the mechanic variables (forces, velocities and positions) are represented as profiles with respect to the wave period. The wave period represents univocally a representative sea-state due to each period value corresponding to a wave height value according to the previous equation. An equivalence between these real sea-states (defined by H_s and T_p values) and a regular wave (defined by its equivalent values of A and T is also established). Thus, real sea-states and its equivalent regular ones have the same total wave-energy, E_w ($E_w = (\rho g/16)H_s^2 = (\rho g/2)A^2$, the average – per unit of area – of the kinetic and potential energy of a sea-state) and wave-power, J_w (wave power or wave energy flux per length of wave front - $J_w = (\rho g^2/(64\pi^2))T_{-1,0}H_s^2 = (\rho g^2/(16\pi^2))TA^2$, where $T_{-1,0} = 0.8572 \cdot T_p$ when assuming a Pierson-Moskowitz wave spectrum), which means the equivalences : $T = 0.8572 \cdot T_p$ and $2\sqrt{2} \cdot A = H_s$ [29]. The regular wave equivalent to each real sea-state has been used in the WEC model in order to reduce the computational complexity of the preliminary dimensioning process. The use of regular waves implies an overestimation of the wec energy extracted value, which should be added to other uncertainties such as the use of a linear-frequency domain model. However, power performance calculations under regular waves can be considered an acceptable approximation [31]–[33] for a preliminary dimensioning method.

Due to the uncontrollable nature of ocean waves, four WEC operational states have been defined (see Fig. 2). In *state I*, wave power is too low for profitable energy extraction, so the operation is not enabled. In *state II*, the maximum energy extraction requires the use of an optimal control. In *state III*, the extracted power is limited to the nominal power. The extreme wave conditions of *state IV* risk WEC performance and require the use of survival mechanisms.

From the sea-sate Occurrence Probability (OP) profiles of the representative sea-states of *Santoña*, it is possible to delimit the operational states (Fig. 3): T_{min} and T_{max} are the periods that contain 90% of wave occurrence (within the states II and III) and T_{nom} is the most probable sea-state period (delimiting state II from state III). These values are shown in TABLE I.

TABLE I
SANTOÑA LOCATION CHARACTERISTICS

Variable	Value
T_{min}	7.98 [s]
$T_{P\,nom}$	10.2 [s]
T_{max}	15.5 [s]

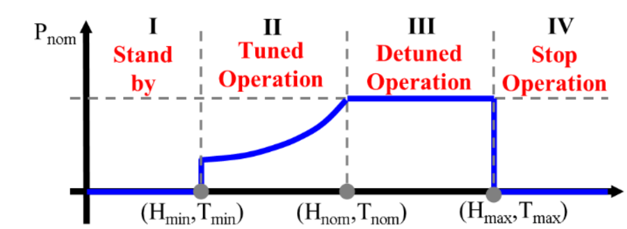

Fig. 2. Operational states of the WEC regarding wave period and wave height.

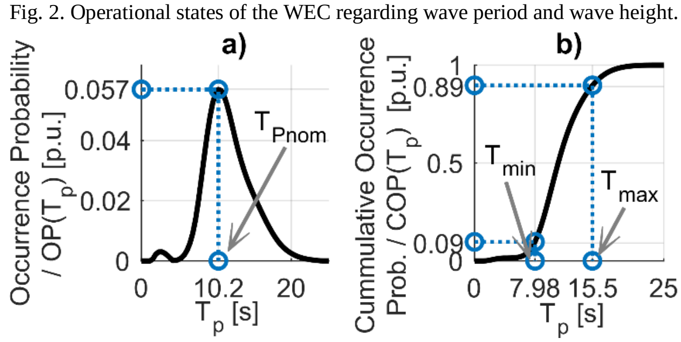

Fig. 3. Occurrence probability and cumulative occurrence probability of the representative sea-states of *Santoña*

B. WEC Dynamic equations

The WEC prime mover concept comprises two bodies: one floating-body (body 1) and one semi-submerged body (body 2). An electrical generator acts as a PTO with its two parts, tied to each WEC body respectively. Fig. 4 shows a diagram of this concept and the forces involved in its movement. By choosing an inertial reference frame and by assuming regular sinusoidal waves, the dynamic frequency-domain equations yields (1) for the body 1 and (2) for the body 2 [29], [34].

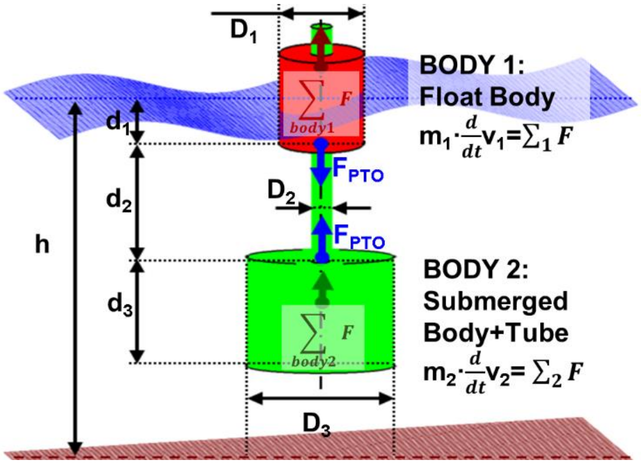

Fig. 4. WEC scheme with geometric definition and dynamic forces involved.

$$[R_{v.1}+R_{v.12}+R_{r11}+S_1/j\omega+j\omega(m_1+m_{ad11})]\hat{v}_1 +[R_{v_{12}}+R_{r12}+j\omega\cdot m_{ad12}]\hat{v}_2 =\ldots \quad (1)$$
$$\ldots = Z_{11}\hat{v}_1+Z_{12}\hat{v}_2 = A\cdot\hat{f}_{e,1}-\hat{F}_{PTO}$$

$$[R_{v_{,2}}+R_{v_{,12}}+R_{r2}+S_2/j\omega+j\omega(m_2+m_{ad22})]\hat{v}_2 +[R_{v_{12}}+R_{r12}+j\omega\cdot m_{ad12}]\hat{v}_1 = \cdots \quad (2)$$
$$\ldots = Z_{12}\hat{v}_1+Z_{22}\hat{v}_2 = A\cdot\widehat{f}_{e,2}+\hat{F}_{PTO}$$

Coefficients R_{r11}, R_{r22}, R_{r12}, m_{ad11}, m_{ad22}, m_{ad12}, $f_{e,1}$ and $f_{e,2}$ are frequency dependent and can be evaluated from the geometry of the WEC prime mover. Their values can be obtained using commercial software tools like WAMIT© or AQWA©, or using semi-analytic solutions for each WEC concept [35].

C. Power Loss Model of the PTO.

The PTO considered is a linear generator [36]. Without prejudice to the generality, the rated characteristics of the PTO, comprised in TABLE II, are based on a real prototype of a switched reluctance linear electric generator (SRLG) [26]. These values and a loss model could be inferred from accessible PTO information in cases with different PTO concepts and different development stages. In the case of a linear generator, its electrical dynamics [37] are faster than WEC mechanical dynamics. Therefore, the force command (F_{PTO}*, determined by the control-strategy, see IV.D) can be considered instantly exerted (considering that F_{PTO}*=F_{PTO}), and the electrical output power can be evaluated from the PTO power losses value and the mechanical output power. A loss model evaluates the losses (including mechanical, iron and copper losses) in the PTO from the values of the mechanical dynamic variables (F_{PTO}, $\hat{v}_1$ and $\hat{v}_2$). In an electric direct drive, the ratio between force and velocity is greater than in conventional rotatory electric generators, which means that forces, and consequently currents (variables practically proportional), reach high values. Thus, copper or *Joule* effect losses are higher than iron losses and mechanical losses (low due to low PTO velocity) and only the former are considered (3) [34], [38].

$$P_{elect}=P_{mec}-P_{cu}=(1/2)\cdot[\hat{F}_{PTO}(\hat{v}_1-\hat{v}_2)-R'\cdot\hat{F}_{PTO}{}^2] =(1/2)\cdot[\hat{F}_{PTO}(\hat{v}_1-\hat{v}_2)-[R\cdot(I^2_{nom}/F^2_{nom})]\cdot\hat{F}_{PTO}{}^2]; \quad (3)$$

TABLE II
PTO CHARACTERISTICS.

Variable	Value [a]
Nominal Power[1] (P_{nom})	200 [kW]
Nominal Force (F_{nom})	200 [kN]
Maximum Velocity (V_{nom})	1.0 [m/s]
Maximum stroke (S_{nom})	4 [m]

[1] P_{nom} is SRLG nominal peak power (the result of multiplying F_{nom} by v_{nom})

D. Energy Extraction Control-Strategy equations

Power generation in a PTO is dependent on the energy extraction control-strategy. It continuously calculates the F_{PTO} value to be imposed by the PTO. Frequency-domain equations of the control strategy are based on an optimal control [29] but modified to consider PTO rated characteristics and PTO losses.

Firstly, the optimal profile of F_{PTO} phasor value ($|F_{PTO}|$ and θ_{PTO}) is evaluated using a *Thevenin* equivalent circuit (right side of Fig. 5) of a WEC analogue electric circuit (left side of Fig. 5). Force, velocity, mass stiffness and damping are analogous to voltage, current, inductance and the inverse of capacitance and resistance respectively [29], [31]. *Thevenin* impedance (Z_T) and voltage (F_T) are evaluated from (4) and (5) respectively. From equations (4)(5), the electrical output power (6) is expressed in terms of F_{PTO} phasor module and angle values.

$$Z_T = (Z_{11}\cdot Z_{22}-Z_{12}{}^2)/(Z_{11}+Z_{22}+2\cdot Z_{12}); \quad (4)$$
$$\hat{F}_T=((Z_{11}+Z_{12})A\hat{f}_{e,1}-(Z_{22}+Z_{12})A\hat{f}_{e,1})/(Z_{11}+Z_{22}+2Z_{12}) \quad (5)$$
$$P_{elect}=(1/|Z_T|)[|\hat{F}_T\cdot\hat{F}_{PTO}|\cos(\theta_{F\_PTO}+\theta_{Z\_T})-\ldots\ldots(|\hat{F}_{PTO}|^2\cos(\theta_{Z\_T})]-R|\hat{F}_{PTO}|^2 \quad (6)$$

Secondly, the F_{PTO} phasor values are calculated maximizing P_{elect} (6) and considering the limitation of the $|F_{PTO}|$ (upper limited by its nominal value, F_{nom}, shown in TABLE II). These equations are obtained by solving a constrained maximization problem by using *Lagrance* multipliers (7)(8).

$$|\hat{F}_{PTO}|=max(F_{nom},(\hat{F}_T\, Z_T^*/(2\cdot R_T+2\cdot R'\cdot|Z_T|^2)|) \quad (7)$$
$$\theta_{F\_PTO}=angle(\hat{F}_T\cdot Z_T^*/(2\cdot R_T+2\cdot R'\cdot|Z_T|^2)|) \quad (8)$$

Finally, a geometrical interpretation of the complex phasor variables is set to consider the PTO velocity and stroke limitations [39]. F_{PTO}, expressed as F_{PTO_x} and F_{PTO_y} components (real and imaginary components of the phasor F_{PTO} respectively) on a two-dimensional space (Fig. 6), leads to the WEC dynamic expressions (9). Equations (10)(11)(12) express, in the same two-dimensional space, the inequalities of the force, velocity and stroke limitations respectively.

$$\hat{F}_T=\hat{F}_{PTO\_x}+j\hat{F}_{PTO\_y}+(R_T+jX_T)(\hat{v}_{r\_x}+j\hat{v}_{r\_y}) \quad (9)$$
$$F_{PTO\_x}{}^2+F_{PTO\_y}{}^2 \leq F_{nom} \quad (10)$$
$$((F_{PTO\_x}-F_{T\_x})^2+(F_{PTO\_y}-F_{T\_y})^2)/|Z_T| \leq v_{nom} \quad (11)$$
$$((F_{PTO\_x}-F_{T\_x})^2+(F_{PTO\_y}-F_{T\_y})^2)/(\omega\bullet|Z_T|) \leq s_{nom}/2 \quad (12)$$

The geometrical interpretation of (10) is a circle with center located at the origin, and the geometrical interpretation of (11)(12) are two concentric circles with their centers displaced from the origin. F_{PTO} value should be in the overlap area of these three circles for each wave frequency, fulfilling the constraints of minimum force and, maximum velocity and stroke. If the optimum value of F_{PTO}, defined by equations (7)(8), fulfills the limitations defined by equations, the optimum energy extraction is feasible (case C in Fig. 7). If it does not, as in case B of Fig. 7, the maximization of energy extraction should be substituted by choosing the feasible PTO force value closest to optimum value in the (F_{PTO_x}, F_{PTO_y}) space. The case A, presented in Fig. 7.a, implies there is no overlap area, i.e. there are no operation points that fulfill the WEC limitations.

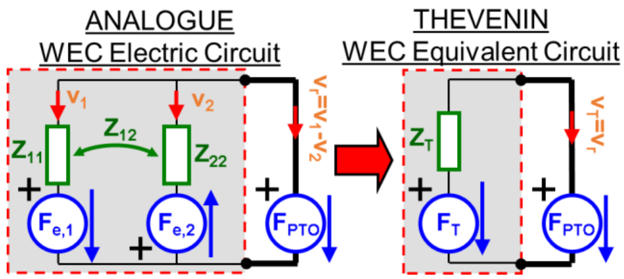

Fig. 5. Analogue electric circuit of the WEC mechanical system (right side) and *Thevenin* equivalent electric circuit (left side).

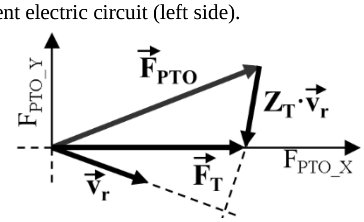

Fig. 6. Geometrical interpretation of the PTO force calculation of (9).

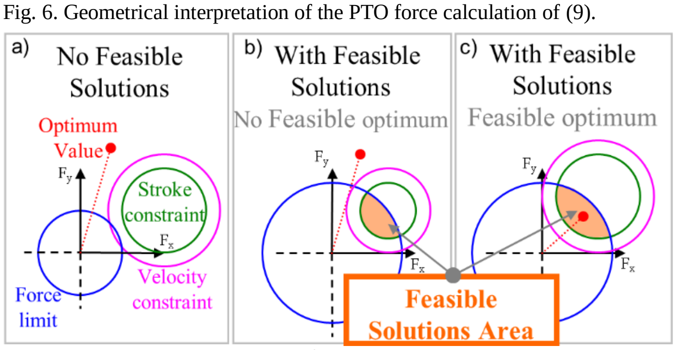

Fig. 7. Geometrical interpretation of control-strategy. Case a): the mechanical system cannot fulfill the constraints of velocity and stroke. Case b) the constraints are fulfilled but energy extraction maximization is not possible. Case c) the energy extraction can be maximized fulfilling the constraints.

V. Wave Energy Converter Dimensioning Problem

The WEC geometry design is represented as a mathematical optimization problem, which requires defining: search space V.A; objective functions V.B; and constraints V.C. Finally, the formulation of the optimization problem is presented in V.D.

A. Search-Space

The search-space delimits the domain of the free variables of the optimization problem. Each set of values for the search-space variables defines one candidate solution, and the values of each variable are changed along the iterations in order to improve the objective functions. Search-space variables define the geometry of the point absorber, which is simplified by using cylindrical bodies. Five variables define the geometry; D_1, D_3, d_1, d_2 and d_3 (see Fig. 4). Value of D_2 does not belong to the search-space, but it is fixed by the external PTO diameter.

B. Objective/cost function

The objective function in an real design problem should be, ideally, a purely economic function [9], [40]. However, in the case of technologies under development, like wave energy, a multi-objective function (considering each objective function individually along with its impact on variables) could give more useful information than a global estimated benefit function. The optimization problem solution is a set of equally optimal solutions so-called *Pareto Frontier* (PF), and the final solution is chosen among them [2], [3], [19].The method considers two objective functions: minimizing the WEC surface (13) and the maximizing annual energy extracted by the WEC (14). These are both evaluated in the frequency domain from the WEC mechanical model. The former is assumed to be related to the cost of materials, moorings, etc. The latter is assumed to be directly related to the profit derived from the energy production. Due to the fidelity of the models used, the energy extracted accuracy could be considered an acceptable approximation for an optimization problem (more focused on the comparison of the power extraction capacity of different solutions than in obtaining a high accuracy).

$$S_{WEC}\,[m^2]=\pi\cdot(D_1\cdot d_1+D_2\cdot d_2+D_3\cdot d_3+0.25\cdot D_1^2 \ldots \\ \ldots+0.5\cdot D_3^2-0.5\cdot D_2^2) \quad (13)$$

$$E[Wh]=\sum_{T=T_{min}}^{T_{max}} P_{elect}(T)\cdot\frac{OP(T_p)}{100}\cdot 365\cdot 24 \quad (14)$$

C. Constraints

The constraints are represented by forbidden areas within the period profiles of mechanical variables. The forbidden areas are delimited by the period ranges of operational states (defined in sub-section IV.A, TABLE I) and the limit values of these mechanical variables. Fig. 8 shows the graphical representation of the three types of constraints used: minimum value constraint (a), maximum value constraint (b) and the case of the resonance constraint (c).

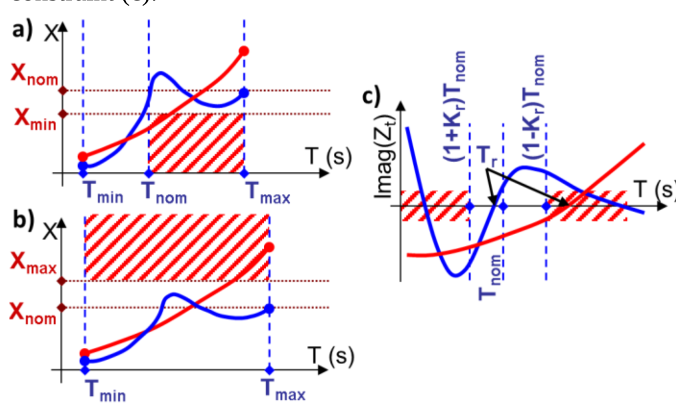

Fig. 8. Optimization problem constraints of the period profile of a generic variable 'X'. (a) Minimum value constraint. (b) Maximum value constraint. (c) Resonance constraint.

In addition, 2 example period profiles of generic mechanical variables are presented: a red profile that crosses the forbidden zone (cross-hatched square) and corresponds to an unfeasible solution; and a blue profile that corresponds to a solution that fulfils the constraint In the case study, Constraints 1), 2) and 3) match the PTO objective characteristics and feasibility limits, and WEC dimensions during the dimensioning process; Constraints for the WEC natural resonance period 4) and slamming 5) ensure the adjustment of the location sea-states to the WEC dimensions. A WEC solution is considered feasible if it fulfills all the 5 constraints, and these constraints include the preliminary accessible information of the project (the framework specifications of the dimensioning problem). The constraints should be adapted depending on issues such as PTO concept or prime mover working principle.

1) Minimum electric generated power,

This constraint is considered in the operational *state III* (15). It ensures the proper PTO power selection to make it work at nominal power for a reasonable wave period range. Its representation with respect to wave period is shown in Fig. 8.a, with variable 'X' representing the generated power.

$$P_{elect}(T) \geq P_{min} = K_P \cdot P_{nom};\ \forall T \in [T_{Pnom}, T_{max}] \quad (15)$$

2) Maximum relative velocity.

Relative velocity of body 1 and body 2 is limited in the operational *states II* and *III* (16). It avoids dangerous situations related to linear bearings (that guide both bodies of the SRLG), as well as to the ability of the end-stop devices to dissipate the mechanical energy if reaches. Its representation is shown in Fig. 8.b with variable 'X' representing the relative velocity.

$$|\hat{v}_1(T) - \hat{v}_2(T)| \leq v_{max} = K_v v_{nom}; \forall T \in [T_{min}, T_{max}] \quad (16)$$

3) Maximum stroke

Relative displacement is constrained in operational *states II* and *III* (17) to avoid impacts between the two bodies (impacts absorbed by the end-stop devices). The representation of the maximum displacement constraint is shown in Fig. 8.b, where the variable 'X' is the stroke.

$$|\hat{s}_1(T) - \hat{s}_2(T)| \leq s_{max} = K_s s_{nom}; \forall T \in [T_{min}, T_{max}] \quad (17)$$

4) WEC resonance.

The natural resonance of the WEC must be close to the period of maximum probability of sea-state occurrence, in order to reduce the reactive power required by the control strategy (and as a result, the PTO). Fig. 8.c represents the constraint as an allowed zone (centered in T_{nom}) for the zero-crossing period of the imaginary part of the WEC impedance Z_T.

$$|T_r - T_{Pnom}| \leq K_r \cdot T_{Pnom};\ imag\big(Z_T(T_r)\big) = 0 \quad (18)$$

5) Anti-Slamming

This constraint ensures the absence of slamming effect in the operational *states II* and *III* (19). It prevents the floating body from getting out of the water or being submerged completely. It is a maximum value type of constraint, Fig. 8.b, where variable '*X*' is distance between the bottom of body 1 and the sea surface.

$$\left|\hat{s}_1(T) - \hat{A}(T)\right| \leq s_{Lmax} = K_{sl} d_1; \forall T \in [T_{min}, T_{max}] \quad (19)$$

More complex adjustment of WEC design could be achieved by adding other constraints such as maximum pitch oscillation or sway movement or maximum stress in moorings [41].

D. Optimization problem formulation.

Once the optimization algorithm is chosen, the mathematical optimization problem can be formulated. A Multi-Objective DE is used due to its qualitative characteristic (commented in III); without prejudice that alternative algorithms would be suitable. WEC dimensioning design is formulated in the standard form of a continuous optimization problem [1] as follows.

- 2 objective functions are minimized: f_1, f_2 (20); see V.B and (13)(14).
- It is subjected to 5 inequality constraints: g_1, g_2, g_3, g_4 and g_5 (21); see V.C and (15)(16)(17)(18)(19).
- The free variable vector (of the search-space, see V.A) has 5dimensions: $X=[x_1, x_2, x_3, x_4, x_5]$ (22).

$$\min_X \begin{cases} f_1(X) = S_{WEC}; \\ f_2(X) = -E; \end{cases} \quad (20)$$

Subject to:

$$\begin{aligned} g_1(X) &= P_{min} - P_{elect}(T) \leq 0;\ \forall T \in [T_{Pnom}, T_{max}] \\ g_2(X) &= |\hat{v}_r(T)| - v_{max} \leq 0;\ \forall T \in [T_{min}, T_{max}] \\ g_3(X) &= |\hat{s}_r(T)| - s_{max} \leq 0;\ \forall T \in [T_{min}, T_{max}] \\ g_4(X) &= |T_r - T_{Pnom}| - K_r T_{Pnom} \leq 0; \\ g_5(X) &= \left|\hat{s}_1(T) - \hat{A}(T)\right| - s_{Lmax} \leq 0;\ \forall T \in [T_{min}, T_{max}] \end{aligned} \quad (21)$$

where: $X = [x_1, x_2, x_3, x_4, x_5] = [D_1, D_3, d_1, d_2, d_3]$ (22)

For evaluating the objective functions and constraints of each trial solution (defined by free variable vector values), the calculation process uses the model described in IV.

1. Objective function f_1 can be directly calculated from the values of the free variable vector X.
2. Hydrodynamic coefficients (R_{vi}, R_{rij}, m_{adij} and $f_{e,i}$), hydrostatic coefficients (S_i) and the rest of the coefficients (m_i) can be calculated from X, and hence, Z_T can be obtained (4) and g_4 can be evaluated (18).
3. From the previous coefficients, F_{PTO} can be calculated by means of (7) and (8) (subject to (10)(11)(12)).
4. With the values of the coefficients and F_{PTO}, the dynamic variables ($\hat{v}_1, \hat{v}_2, \hat{s}_1, \hat{s}_2$) can be calculated from (1)(2) for each frequency, and hence, g_2, g_3 and g_5, can be obtained (16)(17)(19).
5. From the values of F_{PTO} and dynamic variables, P_{elect} can be evaluated (3). By means of the location information (Fig. 3 shows the *OP(T)* profile of the location) and P_{elect} value, objective function f_2 is obtained.

This calculation process corresponds with the step "EVALUATE POPULATION Q_t" in Fig. 1.

VI. Results And Analysis of the Dimensioning Method

Fig. 9.a shows the geometry of 9 *Pareto*-optimal solutions of point absorber geometries corresponding to the case study of *Santoña* and the WEC and the PTO described in section IV. The *Pareto*-optimal values of the optimization variables are shown for the 9 geometries. The results are obtained from a single execution of the methodology, which are selected from a set of 50 executions. This selection is not critical as the Pareto Frontiers (PF) obtained are very similar. The solutions belong to PF obtained from the application of the optimization algorithm, shown in Fig. 9.b. The previously mentioned 9 *Pareto*-optimal solutions are marked over the PF (with a black circle) and its optimal values are shown, together with its identification number (from 1 to 9). Although all the feasible solutions from

the PF are equally optimal, it is possible to distinguish three intervals, easily identified in Fig. 9.b by three segments, where difference will be analyzed.

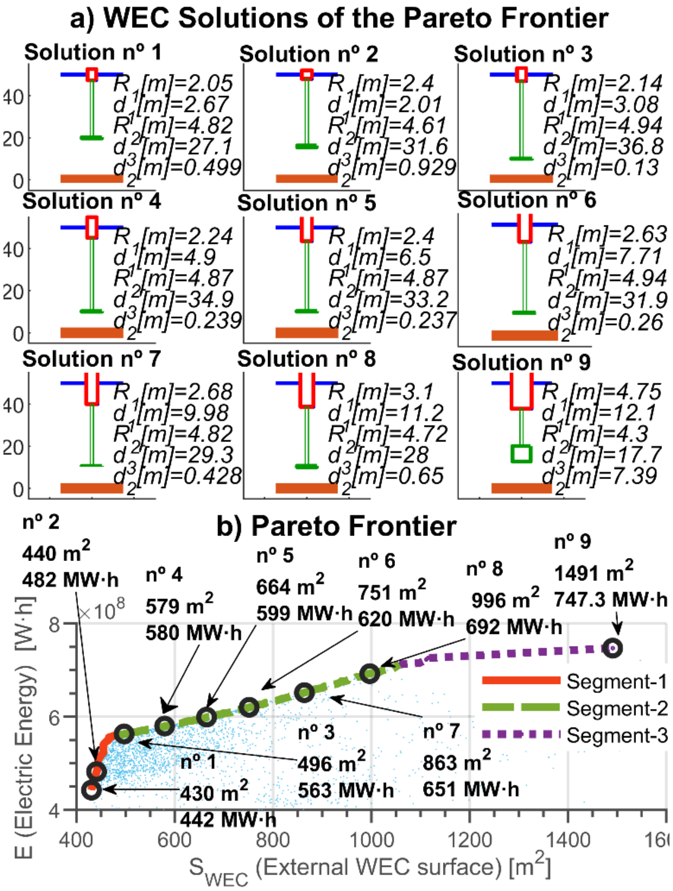

Fig. 9. Results of the preliminary WEC design process. a) Dimensions of 16 WEC solutions from the *Pareto* Frontier. b) *Pareto* Frontier (red, yellow and purple lines and the 16 WEC selected solutions highlighted over it) and feasible WEC solution (blue dots).

In the left zone of the PF (SEGMENT 1, red solid line), the solutions with the lowest amount of material used to build the WEC (surface) are included. In this zone, solutions tend to shorten the spar (d_3) in order to reduce the surface value. This can be a drawback since the spar length reduction and therefore the depth of body 2 (submerged) results in an energy extraction limitation. Medium surface zone solutions (SEGMENT 2, green dashed line) have the submerged body at great depth (and maintains its dimensions relatively stable); while the floating body tends to slightly increase its radius (R_1) and its draft (d_1) more sharply. Finally, high surface solutions (SEGMENT 3, purple dotted line) reduce their ratio energy/surface with respect to the SEGMENT 2 being the investment in surface less profitable in terms of energy.

From data obtained by using the preliminary dimensioning algorithm, the designing process continues by selecting a base solution from the PF to be analyzed and used in further detailed design processes. Although all PF solutions are equally valid from the point of view of the optimization problem resolution, other considerations must be taken into account to select one solution. In absence of more detailed information, the SEGMENT 2 is chosen due to its advantages and within it, the solution 3, which implies that priority is given to the minimization of the WEC surface over the extracted energy. In that sense, any solution close to points where the PF slope starts to decrease, near solution 3, would be an appropriate solution.

In addition, the impact of the definition of the optimization problem in the results of the method has been studied. First, the objective functions (section V.B) of the optimization problem are varied: WEC surface (*Cost Function - 0*) is exchanged by WEC volume (*Cost Function - 1*) as an alternative function that represents WEC cost. The original PF (which optimizes surface) and the alternative PF (which optimizes volume) are represented together with respect to two pairs of objective functions (on one hand, energy and volume; and on the other hand, energy and surface) in Fig. 10.a. Fig. 10.b shows the same PF, but with respect to the WEC dimensions (projections of the 5-dimensional hypersurface on each pair of 2 WEC dimensions).

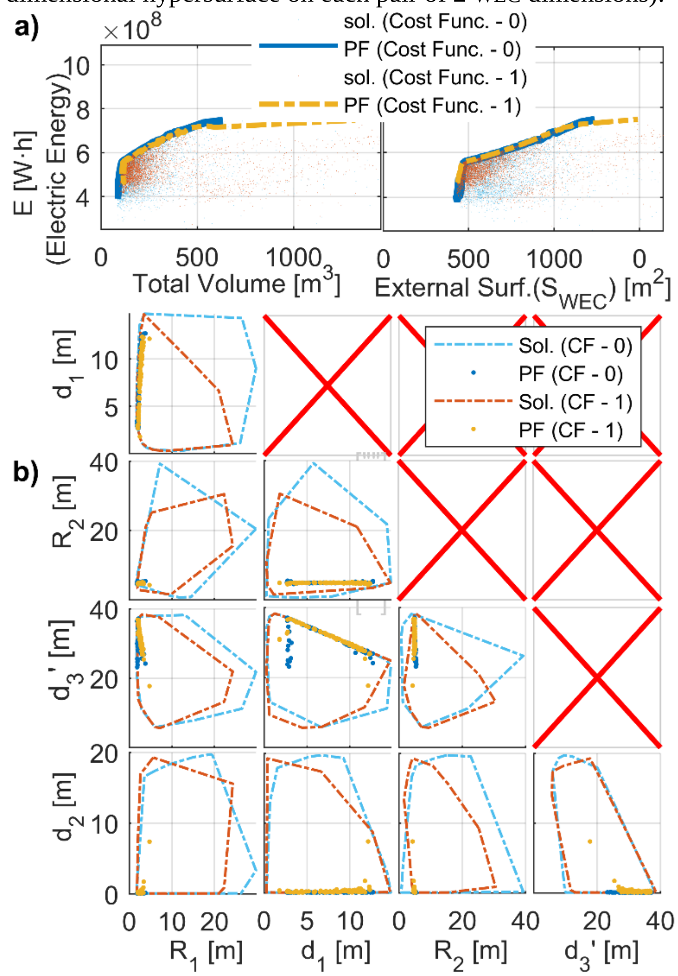

Fig. 10. Comparison of the results of the preliminary WEC dimension design process for two different set of objective functions: WEC surface and WEC volume. a) The *Pareto* frontiers (represented in terms of the objective function) of the two objective function options. b) 2-dimension projection of the 5-dimensions hypervolume representation of the *Pareto* frontier in terms of its dimensions. The dark blue and yellow points represent the WEC solutions of the *Pareto* frontier and the dashed lines delimit the feasible solution zone.

It can be seen how both PFs from Fig. 10.a are very alike in the SEGMENT 2 section, whereas they are different in the sections corresponding to SEGMENTs 1 and 3, which contain less interesting solutions, as pointed out in the previous paragraph.

In these segments, the differences in WEC geometry are associated with differences in the d_3' dimension (heave plate height, Fig. 10.b). An increased d_3' increases more significantly the volume than the surface as the optimization of the surface uses the highest values of this dimension. This increase allows a better tuning of the device natural resonance to the location wave frequencies, due to having a greater mass. Those solutions extract a greater amount of energy (Fig. 10.a, SEGMENT 2).

Second, the constraints are varied; specifically, the original case considers the WEC resonance constraint – section I.A.4) - (*Constraint - 1*) and an alternative case not considering this constraint (*Constraint – 0*) is analyzed. Fig. 11.a shows the two PF vs. objective functions of the original and alternative case. In Fig. 11.b, the same PF are shown in this case with respect to the WEC dimensions. Constraining the WEC natural resonance means to reduce the amount of reactive power provided by the PTO. It is worth remembering the PTO control strategy optimizes P_{elect}, which leads to a limitation in the use of mechanical reactive power, maintaining PTO efficiency in acceptable limits.

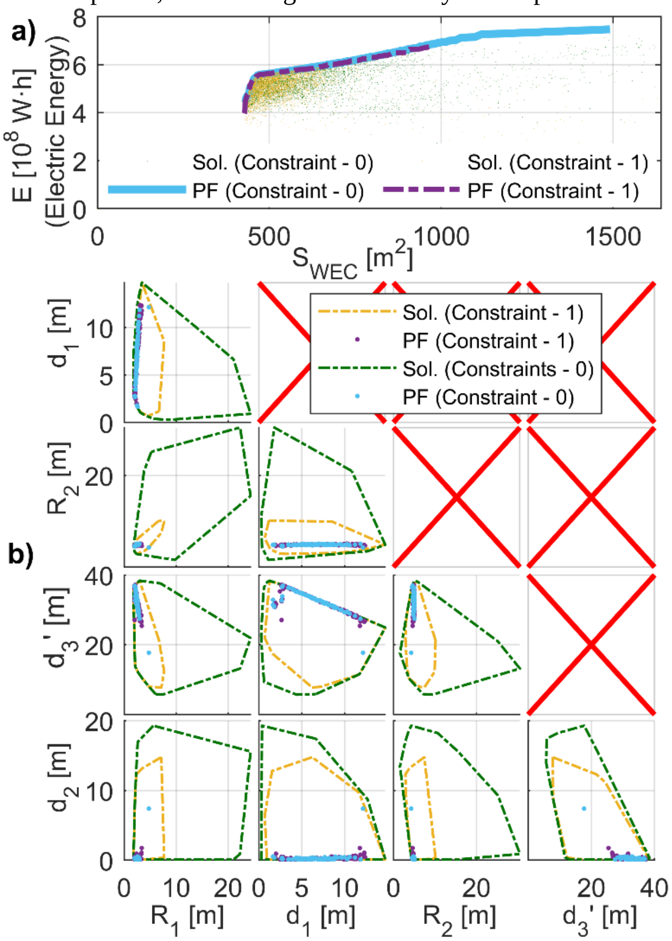

Fig. 11. Comparison of the results of the preliminary WEC dimension design process with the resonant constraint activated and deactivated. a) The *Pareto* frontiers (represented in terms of the objective function). b) 2-dimension projection of the 5-dimensions hypervolume representation of the *Pareto* frontier in terms of its dimensions. The light blue and purple points represent the WEC solutions of the *Pareto* frontier and the dashed lines delimit the feasible solution zone.

Fig. 11.a shows that the two PF, with and without resonance constraint, are mostly coincident. Thus, the best WEC solutions are almost the same. However, there are differences in the space that contains the complete set of analyzed feasible solutions, represented in the dashed lines in Fig. 11.b. Not considering the resonance constraint, widens the searching possibilities. It means that prime mover geometries obtained from the design could have a natural frequency far from (or close to) the specific wave period required for a maximum power transference. That would result in (in the worst case) less energy being absorbed from the waves or more mechanical reactive power being used in order to increase it, leading to higher losses. In summary, this constraint has no great impact in the obtained PF (resonance could increase in importance in locations with lower Wave Energy, lower predominant periods and more concentrated scatter diagram than *Santoña* , as other studies show [5]).

The results of the case study show that the initial definition of the problem has influence on the results obtained in the final design. Thus, the choice of the constraints and the objective functions condition the results (WEC geometry) of surface and energy or, alternatively, of volume and energy, etc.

Consequently, the specific industrial problem to be solved (ballast tanks size, construction materials, type of moorings, PTO technologies to be used, etc.) must be previously analyzed. In addition, this methodology can be improved considering more complex geometries and more detailed design parameters (such as considering more detailed PTO parameters, moorings or power umbilical cable; considering additional constraints such as structural loads or slamming effect, or even improving the model fidelity by means of stochastic models considered in irregular waves). Deeper improvements in the methodology could be tackled by including the PTO rated values in the search space, and dimensioning prime mover and PTO altogether.

These improvements in the dimensioning algorithm would allow reducing the tasks and the calculation effort of the subsequent detailed design process and they will be addressed in future works.

VII. Conclusions

The paper has described in detail a methodology for the preliminary design of the dimensions for wave energy converters (WEC), focused on the case study of a heave point WEC with given Power Take-Off (PTO) technical limitations and required characteristics. The paper provides the guidelines to follow the methodology in order to set a problem of mathematical optimization solved by means of the Differential Evolutionary algorithm. This algorithm considers two objective functions, WEC surface and the annual energy extraction: the former related to capital expenditures, and the latter related to incomes. In addition, it considers a set of constraints given by the WEC, the PTO and the wave climate of the location in *Santoña*, *Spain*.

Considering the methodology integrated in a whole WEC design process, the *Pareto Frontier* (PF) of solutions can be obtained as a result for the case study. The most suitable solution should be selected from the PF set of solutions as the input of the detailed engineering. In absence of more information, the area of highest ratio energy/surface is preferable. However, in the detail engineering process, other considerations such as the PTO characteristics or the total power of the wave energy farm could gain importance and it could modify the WEC geometry selected. Additionally, an analysis of the dependence of the geometry obtained as solutions when the setting of the optimizations problem is modified has been accomplished. On one hand, WEC surface is exchanged with WEC volume as cost function and, on the other hand, the natural resonance constraint is eliminated. Different WEC geometries are obtained modifying the optimization problem, so the translation between the design problem and the optimization problem could condition the results.

The methodology proposed permits the automation of the WEC prime mover dimension design, a key step in the whole design process. This facilitates the WEC design and could improve the results due to the methodology explore geometries without any preconception. Despite the methodology being integrated in a detailed engineering, many parameters can be set, and useful information of the energy production and the investment cost can be derived from its prelaminar results.

VIII. References

[1] A. F. de O. Falcão, “Wave energy utilization: A review of the technologies,” *Renew. Sustain. Energy Rev.*, vol. 14, no. 3, pp. 899–918, Apr. 2010.

[2] A. P. McCabe, “Constrained optimization of the shape of a wave energy collector by genetic algorithm,” *Renew. Energy*, vol. 51, no. n/a, pp. 274–284, Mar. 2013.

[3] A. Kurniawan and T. Moan, “Optimal Geometries for Wave Absorbers Oscillating About a Fixed Axis,” *Ocean. Eng. IEEE J.*, vol. 38, pp. 117–130, 2013.

[4] P. Tokat and T. Thiringer, “Sizing of IPM Generator for a Single Point Absorber Type Wave Energy Converter,” *IEEE Trans. Energy Convers.*, vol. 33, no. 1, pp. 10–19, Mar. 2018.

[5] M. Blanco, P. Moreno-Torres, M. Lafoz, and D. Ramírez, “Design Parameter Analysis of Point Absorber WEC via an Evolutionary-Algorithm-Based Dimensioning Tool,” *Energies*, vol. 8, no. 10, pp. 11203–11233, Oct. 2015.

[6] P. B. Garcia-Rosa and J. V. Ringwood, “On the Sensitivity of Optimal Wave Energy Device Geometry to the Energy Maximizing Control System,” *IEEE Trans. Sustain. Energy*, vol. 7, no. 1, pp. 419–426, Jan. 2016.

[7] S. Das and P. N. Suganthan, “Differential Evolution: A Survey of the State-of-the-Art,” *IEEE Trans. Evol. Comput.*, vol. 15, no. 1, pp. 4–31, Feb. 2011.

[8] B. Zanuttigh, E. Angelelli, A. Kortenhaus, K. Koca, Y. Krontira, and P. Koundouri, “A methodology for multi-criteria design of multi-use offshore platforms for marine renewable energy harvesting,” *Renew. Energy*, vol. 85, pp. 1271–1289, 2016.

[9] V. Piscopo, G. Benassai, L. Cozzolino, R. Della Morte, and A. Scamardella, “A new optimization procedure of heaving point absorber hydrodynamic performances,” *Ocean Eng.*, vol. 116, pp. 242–259, 2016.

[10] C. Liang and L. Zuo, “On the dynamics and design of a two-body wave energy converter,” *Renew. Energy*, vol. 101, pp. 265–274, Feb. 2017.

[11] B. C. Boren, P. Lomonaco, B. A. Batten, and R. K. Paasch, “Design, Development, and Testing of a Scaled Vertical Axis Pendulum Wave Energy Converter,” *IEEE Trans. Sustain. Energy*, vol. 8, no. 1, pp. 155–163, Jan. 2017.

[12] V. Castellucci, J. Garcia-Teran, M. Eriksson, L. Padman, and R. Waters, “Influence of Sea State and Tidal Height on Wave Power Absorption,” *IEEE J. Ocean. Eng.*, vol. 42, no. 3, pp. 566–573, Jul. 2017.

[13] R. Baños, F. Manzano-Agugliaro, F. G. G. Montoya, C. Gil, A. Alcayde, and J. Gómez, “Optimization methods applied to renewable and sustainable energy: A review,” *Renew. Sustain. Energy Rev.*, vol. 15, no. 4, pp. 1753–1766, May 2011.

[14] L. Cuadra, S. Salcedo-Sanz, J. C. C. Nieto-Borge, E. Alexandre, and G. Rodríguez, “Computational intelligence in wave energy: Comprehensive review and case study,” *Renew. Sustain. Energy Rev.*, vol. 58, pp. 1223–1246, May 2016.

[15] Roger Aarenstrup, *Managing Model-Based Design*, 1st ed. CreateSpace Independent Publishing Platform, 2015.

[16] R. P. Gomes, J. C. Henriques, L. M. Gato, and A. F. de O. Falcão, “IPS 2-Body Wave Energy Converter: Acceleration Tube Optimization,” *Int. J. Offshore Polar Eng.*, vol. 20, no. 4, pp. 247–255, 2010.

[17] S. Ambühl, M. Kramer, and J. Sørensen, “Reliability-Based Structural Optimization of Wave Energy Converters,” *Energies*, vol. 7, pp. 8178–8200, 2014.

[18] R. P. F. Gomes, J. C. C. Henriques, L. M. C. Gato, and A. F. de O. Falcão, “Hydrodynamic optimization of an axisymmetric floating oscillating water column for wave energy conversion,” *Renew. Energy*, vol. 44, pp. 328–339, 2012.

[19] J. Cordonnier, F. Gorintin, A. De Cagny, A. H. H. Clément, and A. Babarit, “SEAREV: Case study of the development of a wave energy converter,” *Renew. Energy*, vol. 80, pp. 40–52, Aug. 2015.

[20] A. F. de O. Falcão, J. C. C. Henriques, L. M. C. Gato, and R. P. F. Gomes, “Air turbine choice and optimization for floating oscillating-water-column wave energy converter,” *Ocean Eng.*, vol. 75, pp. 148–156, 2014.

[21] J. Goggins and W. Finnegan, “Shape optimisation of floating wave energy converters for a specified wave energy spectrum,” *Renew. Energy*, vol. 71, pp. 208–220, 2014.

[22] P. B. Garcia-Rosa, G. Bacelli, and J. V. Ringwood, “Control-Informed Optimal Array Layout for Wave Farms,” *IEEE Trans. Sustain. Energy*, vol. 6, no. 2, pp. 575–582, Apr. 2015.

[23] O. Farrok, M. R. Islam, Y. Guo, J. Zhu, and W. Xu, “A Novel Design Procedure for Designing Linear Generators,” *IEEE Transactions on Industrial Electronics*, vol. 65, no. 2, pp. 1846–1854, Feb-2017.

[24] B. Holmes *et al.*, “Sea Trial Manual,” 2011.

[25] P. Ruiz, V. Nava, M. Topper, P. Minguela, F. Ferri, and J. Kofoed, “Layout Optimisation of Wave Energy Converter Arrays,” *Energies*, vol. 10, no. 9, p. 1262, Aug. 2017.

[26] “UNDIGEN information (webpage),” 2015. [Online]. Available: http://www.plocan.eu/images/stories/Proyectos/UNDIGEN_esp.pdf. [Accessed: 14-Jun-2015].

[27] E. Oksuztepe, “In-Wheel Switched Reluctance Motor Design for Electric Vehicles by Using a Pareto-Based Multiobjective Differential Evolution Algorithm,” *IEEE Trans. Veh. Technol.*, vol. 66, no. 6, pp. 4706–4715, Jun. 2017.

[28] A. H. Hansen and H. C. Pedersen, “Optimal configuration of a discrete fluid power force system utilised in the PTO for WECs,” *Ocean Eng.*, vol. 117, pp. 88–98, 2016.

[29] J. Falnes, *Ocean Waves and Oscillating Systems, Linear Interactions Including Wave-Energy Extraction*. Cambridge: Cambridge University Press, 2002.

[30] L. H. Holthuijsen, *Waves in oceanic and coastal waters*. Cambridge University Press, 2007.

[31] L. Hai, M. Goteman, and M. Leijon, “A Methodology of Modelling a Wave Power System via an Equivalent RLC Circuit,” *IEEE Trans. Sustain. Energy*, vol. 3029, no. c, pp. 1–1, Oct. 2016.

[32] A. Albert, G. Berselli, L. Bruzzone, and P. Fanghella, “Mechanical design and simulation of an onshore four-bar wave energy converter,” *Renew. Energy*, vol. 114, pp. 766–774, Dec. 2017.

[33] W. Sheng and T. Lewis, “Energy conversion: A comparison of fix- and self-referenced wave energy converters,” *Energies*, vol. 9, no. 12, p. 1056, Dec. 2016.

[34] M. Penalba and J. Ringwood, “A Review of Wave-to-Wire Models for Wave Energy Converters,” *Energies*, vol. 9, no. 7, p. 506, Jun. 2016.

[35] S. Olaya, J. M. Bourgeot, and M. E. H. Benbouzid, “Hydrodynamic Coefficient Computation for a Partially Submerged Wave Energy Converter,” *Ocean. Eng. IEEE J.*, vol. PP, pp. 1–14, 2014.

[36] J. Faiz and A. Nematsaberi, “Linear electrical generator topologies for direct-drive marine wave energy conversion- an overview,” *IET Renew. Power Gener.*, vol. 11, no. 9, pp. 1163–1176, Jul. 2017.

[37] D. Wang, C. Shao, X. Wang, and C. Zhang, “Performance Characteristics and Preliminary Analysis of Low Cost Tubular Linear Switch Reluctance Generator for Direct Drive WEC,” *IEEE Trans. Appl. Supercond.*, vol. 26, no. 7, pp. 1–5, Oct. 2016.

[38] D.-E. Montoya Andrade, A. de la Villa Jaén, and A. García Santana, “Considering linear generator copper losses on model predictive control for a point absorber wave energy converter,” *Energy Convers. Manag.*, vol. 78, pp. 173–183, Feb. 2014.

[39] G. Bacelli and J. V Ringwood, “A geometric tool for the analysis of position and force constraints in wave energy converters,” *Ocean Eng.*, vol. 65, pp. 10–18, 2013.

[40] B. Teillant, R. Costello, J. Weber, and J. Ringwood, “Productivity and economic assessment of wave energy projects through operational simulations,” *Renew. Energy*, vol. 48, pp. 220–230, Dec. 2012.

[41] J. B. Thomsen, F. Ferri, J. P. Kofoed, and K. Black, “Cost optimization of mooring solutions for large floating wave energy converters,” *Energies*, vol. 11, no. 1, p. 159, Jan. 2018.